Journal of Environmental Management 236 (2019) 715–719

Contents lists available at ScienceDirect

Journal of Environmental Management

journal homepage: www.elsevier.com/locate/jenvman

Research article

Design of an industrial solid waste processing line to produce refuse-derived fuel

Luciano R. Infiesta[a], Cassius R.N. Ferreira[b], Alam G. Trovó[c], Valério L. Borges[b], Solidônio R. Carvalho[b,*]

[a] Carbogás Energia, Avenida Guaraciaba, 659, 09370-840, Mauá, São Paulo, Brazil
[b] Universidade Federal de Uberlândia, Faculdade de Engenharia Mecânica, Avenida João Naves de Ávila, 2121, 38408-100, Uberlândia, Minas Gerais, Brazil
[c] Universidade Federal de Uberlândia, Instituto de Química, Avenida João Naves de Ávila, 2121, 38400-902, Uberlândia, MG, Brazil

ARTICLE INFO

Keywords:
Industrial prototype
Low heating value
Moisture
Renewable energy
Sustainability
Thermal properties

ABSTRACT

Municipal Solid Waste (MSW) from the city of Boa Esperança, Minas Gerais, Brazil, was used to produce refuse-derived fuel (RDF). The MSW contains residues from human society, including product packaging, bottles, batteries, organic waste, fines, textiles, health textiles, plastics, glass, and metals, among others. The following protocol was performed during the conversion of MSW to RDF: (*i*) the raw MSW was placed in a silo and sent to a primary crusher using a metal conveyor belt, which reduced the particle size to 80 mm; (*ii*) the biomass was transferred to a selective waste collection platform by a rubber conveyor belt, and the recyclable waste, metals, and glasses were separated manually; (*iii*) residual metals were removed by a magnetic separator; (*iv*) the waste was transferred to a secondary crusher which reduced the particle size to 60 mm; (*v*) the waste passed through an airborne separator to remove materials with high density, such as glass, stones, and organic materials, using a metallic conveyor belt; (*vi*) the particle size was reduced to 40 mm by a tertiary crusher; (*vii*) the aluminium was separated from the non-metallic materials (plastic, paper, rubber, etc.) using an eddy current separator; (*viii*) the particle size was reduced to 25 mm using a quaternary crusher; (*ix*) the MSW was introduced into a rotary dryer using a metal conveyor belt, where the moisture content was reduced to close to 15 wt%, which required thermal energy equivalent to 186 kWh; (*x*) the RDF was used in a thermochemical reactor and 4148 kWh of thermal energy was produced. In addition, the MSW and RDF were analysed, and the elemental composition and combustion characteristics were determined. Based on these results, the protocol evaluated was found to be effective in the conversion of MSW to RDF, which can be used as a source of renewable fuel.

1. Introduction

Population growth and economic development have significantly increased the rate of municipal solid waste (MSW) generation; it is expected to increase to 2.2 billion ton per year worldwide by 2025. Thus, efforts have been made to solve this environmental problem by reducing and recovering the energy stored in MSW in order to obtain biofuels (Barbosa et al., 2018; Moya et al., 2017).

Different types of biomasses (sugarcane, rice husk, municipal solid waste, wood pellets, wood logs, charcoal, etc.) have been evaluated as sources of renewable energy (Table 1-SM). Although lower values of ash content were obtained for wood pellets and logs, no significant difference was observed between MSW and charcoal, a commercial product. Regarding the calorific values, a similar profile was observed for the various bio-waste solid fuels, whereas charcoal shows a moderately greater high heating value (HHV), with these materials being potential sources of refuse-derived fuel (RDF) (Table 1-SM).

However, the production of high-quality RDF requires a multi-stage waste treatment and separation process, since the heterogeneity and high moisture content of MSW make pre-treatment necessary to enhance its properties as fuel. Common unit operations applied in RDF production are crushing and shredding, classifying and separation of rejects, with the aim of reducing the particle size and separating out materials that can be recycled (ferrous and non-ferrous metals) (Edo et al., 2016; Sarc and Lorber, 2013).

Some studies have demonstrated effective ways to reuse waste as energy in the production of RDF (Aluri et al., 2018; Białowiec et al., 2017; Manyà et al., 2015). However, there are few studies evaluating the use of these technologies at pilot-scale (Násner et al., 2017; Rotheut and Quicker, 2017) and, based on a bibliographic survey, to date no

* Corresponding author.
E-mail address: solidonio@ufu.br (S.R. Carvalho).

https://doi.org/10.1016/j.jenvman.2019.02.017
Received 17 August 2018; Received in revised form 10 January 2019; Accepted 3 February 2019

study has been carried out at industrial scale for a solid waste processing line (SWPL).

Násner et al. (2017) studied the development of RDF in an experimental gasification pilot plant (input of 7.5 tons per day of MSW and output of 2.6 tons per day of RDF) using air as a gasification agent; an economic assessment of the pilot plant implementation was performed and showed that the project was feasible. Rotheut and Quicker (2017) worked on the utilization of RDF from landfill waste processed in a mechanical waste treatment facility for energy production. Considering the additive consumption and combustion performance, co-incineration of landfill-derived RDF with fresh RDF or MSW seems to be appropriate.

Therefore, the current work presents the design of an industrial SWPL capable of converting approximately 55 ton day^{-1} of MSW into 30 ton day^{-1} of RDF. In addition, an economic assessment (energy consumption for RDF production × energy production from the RDF) was performed to show the viability of the SWLP, which will be used in a gasification power plant.

2. Materials and methods

2.1. Solid waste processing line plant design

The MSW was produced by the population of Boa Esperança (21° 05′ 24″ S, 45° 33′ 57″ W), Brazil, a city with 40,000 inhabitants (Instituto Brasileiro de Geografia e Estatística, 2018), and was disposed of in a dump located 3.5 km south of the urban area, with an estimated daily production of 30 ton day^{-1} of MSW.

This work consists of the design of an SWPL (Fig. 1) with class II waste processing for co-processing through thermochemical reactions in accordance with the Brazilian Resolution of the Conselho Nacional do Meio Ambiente no. 316/02 (Conselho Nacional do Meio Ambiente, 2002).

In order to meet environmental safety, treatment, and industrialization requirements, the MSW is processed in a covered and closed shed with a waterproof floor, negative pressure system, and odour control. The waste processing line operates daily for 24 h and processes 55 ton day^{-1} of MSW *in natura*: 30 ton day^{-1} from the city and 25 ton day^{-1} from the dump.

Trucks authorized to enter the SWPL initially move to the weighing site to control the amount of MSW. After weighing, the trucks go to the silo to be unloaded by tipping. The silo was built on the ground and has a power rating of 40 kW, a load capacity of 60 tons, and external dimensions of 18 (length) × 3.5 (width) × 5.45 m (height).

The silo also has a conveyor belt that performs repetitive back and forth movements. The waste takes about 4 h to travel the 18-m length of the silo and move to the next stage of the SWPL. The conveyor belt is drilled for drainage, and the water from the MSW (pre-slurry) is collected. A water pump with a flow rate of 511 kg h^{-1} transfers the pre-slurry to an effluent treatment plant. Treated water is pumped back (flow rate of 1 m^3 h^{-1}) to the collector below the conveyor belt to decrease the odour and viscosity of the pre-slurry.

The primary crusher was designed to receive any type of MSW from the silo without any pre-selection or choice. It has a power rating of 150 kW, and the MSW granulometry at the outlet of the crusher is 80 mm. Its working capacity is 6 ton h^{-1} and it has the following external dimensions: 6 (length) × 1.6 (width) × 0.685 m (height).

During crushing, slurry dripping and water evaporation occur due to the friction of the crusher shaft knives with the residue at the rate of 511 kg h^{-1}. To reduce odours and decrease the viscosity of the collected pre-slurry, water from the effluent treatment plant is injected into the containment tray at a flow rate of 1 m^3 h^{-1}.

All crushed residue falls onto a metal conveyor belt below the crusher. It should be noted that the process is automatic and exempt from human intervention. The SWPL also has alarms that warn in case of failures and stop the equipment in case of emergency.

According to Brazilian Law 12,305/10, the implementation of selective waste collection is a municipal obligation and must be included in any integrated solid waste management plan. Therefore, a waste collection platform was designed (Fig. 1-SM). It allows manual separation and collection of recyclable waste such as ferrous and nonferrous metals, glass, plastics, and others.

A rubber conveyor belt with support plates, a transfer capacity of up to 8 ton h^{-1}, speed of 0.1 m s^{-1}, and inclination of 45° was installed under a metal platform with dimensions of 12 (length) × 1.2 (width) × 0.4 m (height). The support plates fixed to the conveyor belt guarantee transport of the waste without rolling. Eight operators (collectors) are responsible for selecting the desired waste, which is sent to the recyclable containers via four ducts.

A magnetic separator was located at the end of the rubber conveyor belt for the purpose of removing ferrous metals that were not removed by selective collection workers. It was designed to operate in a suspended manner and was positioned transverse to the conveyor belt. The equipment has a power rating of 1.5 kW and a separation capacity of 0.3 ton h^{-1}. Its external dimensions are 1.067 (length) × 0.990 (width) × 0.381 m (height).

The secondary crusher is designed to reduce the particle size of the

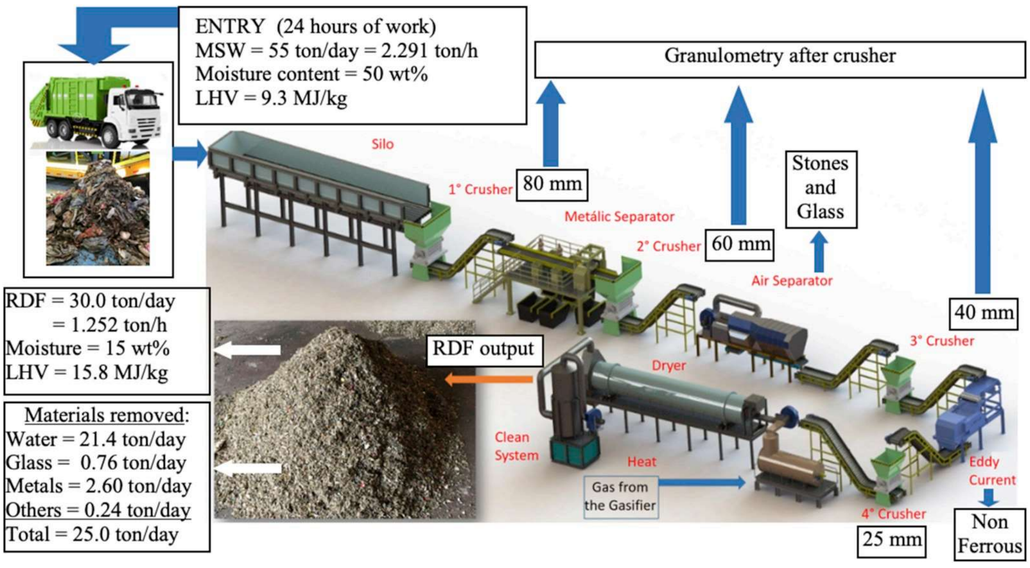

Fig. 1. Scheme of the SWPL.

MSW to 60 mm by rotating two axes with interleaved knives. It has a low rotation rate and high torque, a power rating of 150 kW, a working capacity of 6 ton h^{-1}, and external dimensions of 5.7 (length) × 1.6 (width) × 0.685 m (height).

The MSW with a particle size of 60 mm is moved by a metal conveyor belt into an air separator (Fig. 2-SM) to remove high-density materials, such as glass, stones, piles, and other non-organic materials, and the continuous flow of air from a centrifugal fan maintains the velocity of the air above that required for the pneumatic transport of low-density waste, such as plastics, paper, organic materials, and so on. Moisture removal also occurs in this equipment at a rate of 127 kg h^{-1} due to the passage of the air stream through the crushed waste. The air separator has a power rating of 24 kW and its production capacity is 6 ton h^{-1}. The extraction capacity is up to 500 kg h^{-1} of high-density wastes, which are sent to the extraction container.

After the air separator, a metal conveyor belt carries the MSW to the tertiary crusher, which reduces the size of the waste to 40 mm. The equipment has two axes with rotating intercalated knives, a power rating of 1 × 22 kW plus 1 × 18.4 kW, a working capacity of 6 ton h^{-1}, and the following external dimensions: 3.0 (length) × 1.4 (width) × 2.3 m (height).

After the tertiary crusher, the MSW with a particle size of 40 mm is prepared to pass through the non-ferrous metals separator, called an eddy current separator (Fig. 3-SM). In its first stage, there is a vibrating track with a magnetic roller that captures the metallic remnants that were not captured in the previous processes. In the second stage, there is an electromagnet that generates a magnetic field that repulses non-ferrous metals, such as copper and aluminium. The eddy current equipment has a power rating of 6.6 kW and its production capacity is 6 ton h^{-1}.

The MSW is then transferred by a metal conveyor belt and is inserted by gravity feed into the quaternary crusher. At this stage, residues with a particle size of 40 mm and a mass flow rate of 6 ton h^{-1} are ground and standardized to a mean particle size of 25 mm.

Fig. 4-SM shows the horizontal tubular rotary dryer. The furnace performs combustion of the synthesis gas from the thermochemical waste reactor to generate heat for the rotary dryer.

A metal conveyor belt with 150-mm-tall logs carries the waste to the horizontal tubular rotary dryer, which dries the wet MSW as well as homogenizing it. This equipment has the following technical characteristics:

- Power rating of gear motors: 4 × 3.7 kW,
- Working capacity: 6 ton h^{-1},
- External dimensions: 16 (length) × 2.2 (width) × 5.1 m (height),
- Dryer internal diameter: 1.900 m,
- Input moisture content: 30 wt%,
- Output moisture content: 15 wt%,
- Input air temperature: 400 °C,
- Output air temperature: 80 °C,
- Gas flow through the dryer: 1551.28 Nm^3 h^{-1},
- Weight: 4600 kg.

The scrubber washer is used to remove particulates, moisture, and odours from the hot air exiting the dryer.

In the dryer, MSW with a moisture content of 30 wt% passes through a horizontal tube, which is permeated by hot air at 400 °C generated from the combustion of the synthesis gas in the furnace. This process reduces the moisture content of the waste to 15 wt%; that is, it draws water out at a rate of about 400.7 kg of water per hour. The dryer also has the function of mixing and homogenizing the RDF in order to produce a uniform fuel. The RDF with a moisture content of 15 wt% is discharged onto a metal conveyor belt below the rotary dryer to be transported to the stock warehouse, which has the capacity to store 1000 tons of RDF for future use. In the absence of bulk RDF, the stock of fuel stored in the shed can be used for energy production.

The specifications of the drying and compacting processes are as follows:

- Mass flow of RDF through the dryer: 1252 kg h^{-1},
- RDF granulometry: 25 mm,
- RDF moisture content: 15 wt%,
- RDF density: 250 kg m^{-3}.
- The RDF is carried by a metal conveyor to the receiving hopper of the thermochemical reactor, which converts the RDF into 3235 kg h^{-1} of synthesis gas (syngas) via a gasification process. The thermochemical reactor will be the subject of future work.

Fig. 4-SM also presents the mass and energy balance in the rotary dryer. Neglecting the combustion process and considering only the intake of hot air (400 °C) and RDF with a moisture content of 30 wt% in the dryer, the first system (Eqs. (1) − (3)) to be solved refers to the mass balance of dry RDF:

$$\dot{m}_{RDF_{in}} = \dot{m}_{RDF_{out}} \tag{1}$$

$$\dot{m}_{RDF_{in}} = \dot{m}_{RDF_{30\%}}(1 - 0.3) \tag{2}$$

$$\dot{m}_{RDF_{out}} = \dot{m}_{RDF_{15\%}}(1 - 0.15) \tag{3}$$

where $\dot{m}_{RDF_{in}}$ and $\dot{m}_{RDF_{out}}$ represent the mass of dry RDF at the inlet and outlet of the dryer; $\dot{m}_{RDF_{30\%}}$ represents the mass of RDF with 30 wt% moisture; $\dot{m}_{RDF_{15\%}}$ is presented in Fig. 1 and represents the mass of RDF with 15 wt% moisture (ton h^{-1}).

The second system (Eqs. (4) − (6)) to be solved refers to the mass balance of dry air:

$$\dot{m}_{dry\_Air_{in}} = \dot{m}_{dry\_Air_{out}} \tag{4}$$

$$\dot{m}_{Air_{in}} = \dot{m}_{dry\_Air_{in}} + \dot{m}_{water\_Air_{in}} \tag{5}$$

$$w_{Air_{in}} = \frac{\dot{m}_{water\_Air_{in}}}{\dot{m}_{dry\_Air_{in}}} = \frac{0.622P_v}{P - P_v} \tag{6}$$

where $\dot{m}_{dry\_Air_{in}}$ and $\dot{m}_{dry\_Air_{out}}$ represent the mass of dry air at the inlet and outlet of the dryer; $\dot{m}_{Air_{in}}$ represents the total mass of air (1551.28 Nm^3 h^{-1}) which enters the rotary dryer; $\dot{m}_{water\_Air_{in}}$ represents the mass of water vapour considering that atmospheric air has 60% humidity; $w_{Air_{in}}$ represents the specific humidity (tons of water vapour per ton of dry air); P is the total pressure, and P_v is the pressure of water vapour (Çengel and Boles, 2012).

The third system (Eqs. (7) − (9)) to be solved refers to the mass balance of water:

$$\dot{m}_{water\_RDF_{in}} + \dot{m}_{water\_Air_{in}} = \dot{m}_{water\_RDF_{out}} + \dot{m}_{water\_Air_{out}} \tag{7}$$

$$\dot{m}_{water\_RDF_{in}} = \dot{m}_{RDF_{30\%}} * 0.3 \tag{8}$$

$$\dot{m}_{water\_RDF_{out}} = \dot{m}_{RDF_{15\%}} * 0.15 \tag{9}$$

where $\dot{m}_{water\_Air_{in}}$ was previously calculated from the system composed of Eqs. (4)–(6); $\dot{m}_{water\_RDF_{in}}$ and $\dot{m}_{water\_RDF_{out}}$ represent the amount of water in the RDF before and after the dryer. Thus, $\dot{m}_{water\_Air_{out}}$ can be calculated and represents the mass of water vapour removed from the RDF.

From the mass balance (Eqs. (1)–(9)) and using the first law of thermodynamics in the rotary dryer (Eq. (10)), it is possible to determine the amount of energy required to carry out the drying process of the RDF:

$$\begin{aligned}\dot{Q} + \left[\dot{m}_{RDF_{in}} C_p T\right]_0^{25^\circ C} + \left[\dot{m}_{water\_RDF_{in}} h_{water}\right]_0^{25^\circ C} + \left[\dot{m}_{dry\_Air_{in}} h_{Air}\right]_0^{400^\circ C} \\ + \left[\dot{m}_{water\_Air_{in}} h_{water\_vapor}\right]_0^{400^\circ C} = \left[\dot{m}_{RDF_{out}} C_p T\right]_0^{80^\circ C} \\ + \left[\dot{m}_{water\_RDF_{out}} h_{water}\right]_0^{80^\circ C} \\ + \left[\dot{m}_{dry\_Air_{out}} h_{Air}\right]_0^{80^\circ C} \\ + \left[\dot{m}_{water\_Air_{out}} h_{water\_vapor}\right]_0^{80^\circ C}\end{aligned} \tag{10}$$

Table 1
Mass balance in the waste processing line and calculation/estimation of the average LHV of MSW and RDF.

Composition	Samples				
	MSW (50 wt% moisture)			RDF (15 wt% moisture)	
	Weight (%)	Mass flow ($kg\ h^{-1}$)	LHV ($MJ\ kg^{-1}$)	Mass flow ($kg\ h^{-1}$)	LHV ($MJ\ kg^{-1}$)
Organic waste	35.2	806.7	3.3	474.5	5.6
Fines	3.0	68.8	0.3	40.4	0.5
Paper	6.4	147.8	0.5	86.9	0.8
Packaging	6.0	137.5	0.5	80.9	0.8
Synthetics	8.8	200.5	0.9	118.0	1.6
Textiles	10.0	229.2	1.0	134.8	1.6
Health textiles	12.2	281.9	1.1	165.8	1.9
Plastics	8.8	201.7	1.5	118.6	2.5
Glass	1.4	32.1	0.0	0.0	0.0
Metals	5.2	119.2	0.0	0.0	0.0
Not classified	2.9	66.4	0.2	32.4	0.5
Total	100	2291.8	9.3	1252.3	15.8

where $\dot{Q}$ represents the unknown thermal energy (kW) required by the rotary dryer; C_p represents the specific heat of the RDF ($C_p = 0.9637\ kJ/kgK$); h_{water} represents the enthalpy of water contained in the RDF at the inlet and outlet of the dryer; h_{Air} represents the enthalpy of air at the inlet and outlet of the dryer; h_{water_vapor} represents the enthalpy of water vapour in the air at the inlet and outlet of the dryer; and the air, RDF, and water masses can be calculated by Eqs. (1)–(9).

2.2. Chemical analyses

Potassium and sodium determinations were performed according to EPA Method 3050B (U.S. EPA, 1996), while fluoride and chlorine determinations followed EPA Method 5050 (U.S. EPA, 1994).

Sulfur determinations were done according to ASTM 4239 − 18 (ASTM, 2018), the elemental analysis (CHN) according to ASTM 5373 − 14 (ASTM, 2014), and the oxygen content by difference: [100 − (C + H + N + S)]. The low heating value (LHV) and HHV were determined according to ASTM 5865 − 13 (ASTM, 2013).

Moisture content was determined according to NBR 8389/84 (ABNT, 1984), while the ash content was determined according to an adapted methodology of NBR 9092/2014.

All analyses were performed by the Associação Brasileira de Cimento Portland, a Brazilian laboratory accredited according to the International Organization of Standardization/International Electrotechnical Commission (ISO/IEC) 17025 standard.

3. Results and discussion

Some valuable waste components, such as recyclable plastic, paper, electronics, glass, and metal, are often selected and taken by informal collectors from Boa Esperança; hence only the remaining waste components can be converted into synthesis gas and energy. The combined properties of these remaining waste components were calculated to predict the LHV of the MSW (with 50 wt% moisture) and RDF (with 15 wt% moisture) as shown in Table 1.

The MSW and RDF components were dominated by organic waste followed by textiles, plastics, papers, and others (Table 1). A significant mass loss occurred during the production of RDF 15 wt% (Table 1), which is justified by mechanical and manual treatments applied during the generation of the RDF (Fig. 1). In addition, by decreasing the moisture content by 70% (from 50 to 15 wt%), it was possible to increase the energy content in proportion to the quantity of fuel generated, from 9.3 to 15.8 $MJ\ kg^{-1}$ (Table 1). A similar behaviour was observed upon the application of different mechanical treatments to MSW (Edo et al., 2016).

The electrical energy consumption required to convert MSW to RDF was also determined in accordance with the specifications of the equipment shown in Fig. 1. Therefore, the SWPL would consume around 334 kWh if operated at full capacity. However, the system was designed to operate at only 60% of the maximum electrical capacity. Therefore, 200 kWh is consumed by the SPWL, while the power plant was designed to generate 1500 kWh of electrical energy. It should be noted that the power plant consists of a steam power unit that uses the syngas as fuel. The steam power plant as well as the thermochemical reactor will be themes for future work.

In the design of the rotary dryer (Fig. 4-SM) a thermal efficiency of 75% was adopted. Thus, the drying process will consume 186 kWh of thermal energy while the thermochemical reactor produces about 4148 kWh (Eq. (11)), which demonstrates the feasibility of the SWPL.

$$\dot{Q}_{reactor} = LHV_{syngas}\cdot\dot{m}_{syngas}\cdot 0.8 \tag{11}$$

where $\dot{Q}_{reactor}$ represents the thermal energy produced by the combustion of the syngas considering a thermal efficiency of 80%, LHV_{syngas} represents the low heating value of the synthesis gas (4880 $kJ\ kg^{-1}\ K^{-1}$), and $\dot{m}_{syngas}$ is the mass flow of syngas produced by the thermochemical reactor (3235 $kg\ h^{-1}$).

In addition, the RDF obtained presents a moisture content of only 15 wt%, which is better than the ideal (< 50 wt%) and permits its direct use in a gasification power plant without any addition of fuel (Pasek et al., 2013). Added to that, this RDF can be stored for three or four months because the low moisture content inhibits enzymatic reactions and the growth of microorganisms such as bacteria, fungi, and yeasts (Miller and Clesceri, 2002).

Characterization of the RDF was also performed to verify the properties of the biofuel obtained from isolated or combined municipal and landfill waste (Table 2). As the sodium, potassium, and chlorine contents were low (0.21–1.5 wt%, Table 2), a low contribution to corrosion and saponification could be expected when these materials were used as fuels (Sedenho et al., 2013). Besides, the sulfur content is less than 0.11% (Table 2), which is lower than the average sulfur content in coal (0.23–0.93%) (Liu et al., 2018). The nitrogen content (0.81–1%) showed a similar behaviour (Table 2). In addition, the average content of chlorine contained in the waste fuel was 0.87% (Table 2), a value within the range of biomass fuels (Edo et al., 2016). The sulfur and chlorine contents are harmless concentrations because they are below 0.3 and 1.0%, respectively (Puddy, 1992). Added to this, as the nitrogen and sulfur contents were low in all the fuels, low SO_x and NO_x emissions are expected when using these materials as fuel (Edo et al., 2016).

Table 2
Characterization of the RDF produced from isolated or combined municipal and landfill waste.

Parameter (Unit)	Mass composition		
	100% municipal waste	100% landfill waste	50% municipal and 50% landfill waste
Potassium (wt%)	0.27	0.42	0.32
Sodium (wt%)	0.21	0.33	0.26
Fluoride (wt%)	$< 5 \times 10^{-5}$	7×10^{-3}	8×10^{-3}
Sulfur (wt%)	0.10	0.11	0.11
$LHV_{drybasis}$ ($MJ\ kg^{-1}$)	13.2	14.8	15.8
$HHV_{drybasis}$ ($MJ\ kg^{-1}$)	14.8	16.3	17.2
Nitrogen (wt%)	0.81	0.81	1
Hydrogen (wt%)	8	7	7
Carbon (wt%)	58	47	57
Oxygen (wt%)	34	45	35
Chlorine (wt%)	0.49	1.5	0.62
Ash (wt%)	15	27	26
Moisture (wt%)	25	9.9	15

Similar results were obtained during a feasibility study of the recovery of energy from MSW to generate electricity (Pasek et al., 2013; Edo et al., 2016).

In parallel, the heating values were calculated (Table 2). In order to facilitate the comparison between different biofuels, the relationships between the carbon, hydrogen, and oxygen atoms must be used (Huang et al., 2009). Therefore, comparing the results presented in Table 1-SM for wood with the results in Table 2, there is great similarity in the H/C and O/C ratios, indicating that the heating values of the wood and the MSW evaluated are quite similar.

The average HHV ($16.1 \pm 1.2\,MJ\,kg^{-1}$) and LHV ($14.6 \pm 1.3\,MJ\,kg^{-1}$) obtained in the present work are also in accordance with values presented in the scientific literature, as are the average ash (23 ± 7 wt%) and moisture (17 ± 8 wt%) contents (Table 2). As an example, Wang et al. (2018) used four different solid wastes (dog manure, horse manure, apple pomace waste, and tea waste) and an industrial by-product (NovoGro) to produce solid fuel pellets. According to the authors, the material obtained exhibited excellent mechanical and thermal properties, including an HHV of $16.9 \pm 0.9\,MJ\,kg^{-1}$, an LHV of $12.8 \pm 1.1\,MJ\,kg^{-1}$, an ash content of 19 ± 0.8 wt%, and a moisture content of 12.3 ± 2.3 wt%. In addition, results similar to those presented in Table 2 were obtained in a study performed in Itajubá (22° 25′ 32″ S, 45° 27′ 10″ W), a Brazilian city with about 90,000 inhabitants located 250 km from Boa Esperança.

Regarding the ash content in the immediate analyses, the high values presented in Table 2 are attributed to the presence of sand or soil, mainly in the waste from the landfill. High ash contents in wastes from rubber (23 wt%), synthetics (15 wt%), paper (13 wt%), organics (8 wt%), plastics (5 wt%), and urban pruning (7 wt%) have also been reported in the literature (Pasek et al., 2013).

4. Conclusions

This work demonstrates the design and construction of an industrial prototype SWPL with the capacity to process 55 ton day^{-1} of MSW with a moisture content of up to 50 wt%. In addition, it was possible to produce about 30 ton day^{-1} of RDF with an average moisture content of 17 ± 8 wt% and average LHV of $14.6 \pm 1.3\,MJ\,kg^{-1}$. Based on these results, the RDF produced can be used as biofuel in a gasification power plant without using additional solid or fossil fuel.

The consumption of electrical energy to convert MSW into RDF was determined (200 kWh) and is about 14% of the total electrical energy produced by the thermal power plant (1500 kWh). The thermal energy consumed in the rotary dryer (186 kWh) is about 4.5% of the thermal energy produced by the thermochemical reactor (4148 kWh). Such characteristics demonstrate the feasibility of the SWPL proposed in this work.

Finally, an industrial SWPL and gasification power plant with the capacity to process up to 55 ton day^{-1} of MSW are under construction in the city of Boa Esperança, with an estimated production of 1.5 MWh of electricity.

Conflicts of interest

There are no conflicts to declare.

Acknowledgements

The authors thank the Brazilian companies Furnas Centrais Elétricas S.A. and Carbogás Energia Ltda. and also the government agencies Agência Nacional de Energia Elétrica, Coordenação de Aperfeiçoamento de Pessoal de Nível Superior, Conselho Nacional de Desenvolvimento Científico e Tecnológico, and Fundação de Amparo à Pesquisa do Estado de Minas Gerais for their financial support.

Appendix A. Supplementary data

Supplementary data to this article can be found online at https://doi.org/10.1016/j.jenvman.2019.02.017.

References

ABNT, 1984. Coque – Determinação da umidade total – Método de ensaio. https://www.abntcatalogo.com.br/norma.aspx?ID=10068, Accessed date: 10 December 2018.
ASTM, 2013. Standard Test Method for Gross Calorific Value of Coal and Coke. https://compass.astm.org/EDIT/html_annot.cgi?D5865+13, Accessed date: 10 December 2018.
ASTM, 2014. Standard Test Methods for Determination of Carbon, Hydrogen and Nitrogen in Analysis Samples of Coal and Carbon in Analysis Samples of Coal and Coke. https://compass.astm.org/Standards/HISTORICAL/D5373-14.htm, Accessed date: 10 December 2018.
ASTM, 2018. Standard Test Method for Sulfur in the Analysis Sample of Coal and Coke Using High-Temperature Tube Furnace Combustion. https://compass.astm.org/EDIT/html_annot.cgi?D4239+18e1, Accessed date: 10 December 2018.
Aluri, S., Syed, A., Flick, D.W., Muzzy, J.D., Sievers, C., Agrawal, P.K., 2018. Pyrolysis and gasification studies of model refuse derived fuel (RDF) using thermogravimetric analysis. Fuel Process. Technol. 179, 154–166. https://doi.org/10.1016/j.fuproc.2018.06.010.
Barbosa, F.V., Teixeira, J.C.F., Vilarinho, M.C.L.G., Araujo, J.M.M.G., 2018. Gasification of RDF from MSW – an overview. In: Proc. 4th Int. Conf. Wastes – Solutions, Treatments and Opportunities, pp. 331–338 2018, Porto, Portugal.
Białowiec, A., Pulka, J., Stępień, P., Manczarski, P., Gołaszewski, J., 2017. The RDF/SRF torrefaction. An effect of temperature on characterization of the product – carbonized refuse derived fuel. Waste Manag. 70, 91–100. https://doi.org/10.1016/j.wasman.2017.09.020.
Conselho Nacional do Meio Ambiente, 2002. Resolução CONAMA nº 316, de 29 de outubro de 2002. http://www.mma.gov.br/port/conama/legiabre.cfm?codlegi=338, Accessed date: 17 July 2018.
Çengel, Y.A., Boles, M.A., 2012. Thermodynamics, seventh ed. McGraw-Hill.
Edo, M., Budarin, V., Aracil, I., Persson, P.E., Jansson, S., 2016. The combined effect of plastics and food waste accelerates the thermal decomposition of refuse-derived fuels and fuel blends. Fuel 180, 424–432. https://doi.org/10.1016/j.fuel.2016.04.062.
Huang, C., Han, L., Yang, Z., Liu, X., 2009. Ultimate analysis and heating value prediction of straw by near infrared spectroscopy. Waste Manag. 29, 1793–1797. https://doi.org/10.1016/j.wasman.2008.11.027.
Instituto Brasileiro de Geografia e Estatística, 2018. Brazilian Institute of Geography and Statistics. https://cidades.ibge.gov.br/brasil/mg/boa-esperanca/panorama, Accessed date: 13 July 2018.
Liu, Y., Fan, W., Wu, X., Zhang, X., 2018. Chlorine-induced high-temperature corrosion of boiler steels combusting Sha Erhu coal compared to biomass. Energy Fuels 32, 4237–4247. https://doi.org/10.1021/acs.energyfuels.7b03143.
Manyà, J.J., García-Ceballos, F., Azuara, M., Latorre, N., Royo, C., 2015. Pyrolysis and char reactivity of a poor-quality refuse-derived fuel (RDF) from municipal solid waste. Fuel Process. Technol. 140, 276–284. https://doi.org/10.1016/j.fuproc.2015.09.014.
Miller, P., Clesceri, N.L., 2002. Waste Sites as Biological Reactors: Characterization and Modelling, first ed. Lewis Publishers, Boca Raton.
Moya, D., Aldás, C., Lópes, G., Kaparaju, P., 2017. Municipal solid waste as a valuable renewable energy resource: a worldwide opportunity of energy recovery by using waste-to-energy technologies. In: Proc. 9th Int. Conf. Sustainability in Energy and Buildings, SEB-17, July 2017, Chania, Crete, Greece, pp. 5–7.
Násner, A.M.L., Lora, E.E.S., Palacio, J.C.E., Rocha, M.H., Restrepo, J.C., Venturini, O.J., Ratner, A., 2017. Refuse Derived Fuel (RDF) production and gasification in a pilot plant integrated with an Otto cycle ICE through Aspen plusTM modelling: thermodynamic and economic viability. Waste Manag. 69, 187–201. https://doi.org/10.1016/j.wasman.2017.08.006.
Pasek, A.D., Gultom, K.W., Suwono, A., 2013. Feasibility of recovering energy from municipal solid waste to generate electricity. J. Eng. Technol. Sci. 45, 241–256. https://doi.org/10.5614/j.eng.technol.sci.2013.45.3.3.
Puddy, J.W., 1992. Steam: its Generation and Use, fortieth ed. The Babcock & Wilcox Co., New York.
Rotheut, M., Quicker, P., 2017. Energetic utilisation of refuse derived fuels from landfill mining. Waste Manag. 62, 101–117. https://doi.org/10.1016/j.wasman.2017.02.002.
Sarc, R., Lorber, K.E., 2013. Production, quality and quality assurance of refuse derived fuels (RDFs). Waste Manag. 33, 1825–1834. https://doi.org/10.1016/j.wasman.2013.05.004.
Sedenho, G.C., Paim, L.L., Stradiotto, N.R., 2013. Simple and direct potentiometric determination of potassium ions in biodiesel microemulsions at a glassy carbon electrode modified with nickel(II) hexacyanoferrate nanoparticles. Anal. Methods 5, 4145–4151. https://doi.org/10.1039/C3AY40774H.
U.S. EPA, 1994. Method 5050: Bomb Preparation Method for Solid Waste. https://www.epa.gov/hw-sw846/sw-846-test-method-5050-bomb-preparation-method-solid-waste, Accessed date: 10 December 2018.
U.S. EPA, 1996. Method 3050B: Acid Digestion of Sediments, Sludges, and Soils. https://www.epa.gov/homeland-security-research/epa-method-3050b-acid-digestion-sediments-sludges-and-soils, Accessed date: 10 December 2018.
Wang, T., Li, Y., Zhang, J., Zhao, J., Liu, Y., Sun, L., Liu, B., Mao, H., Lin, Y., Li, W., Ju, M., Zhu, F., 2018. Evaluation of the potential of pelletized biomass from different municipal solid wastes for use as solid fuel. Waste Manag. 74, 260–266. https://doi.org/10.1016/j.wasman.2017.11.043.